NASA TECHNICAL MEMORANDUM

NASA TM X-71474

NASA TM X-71474

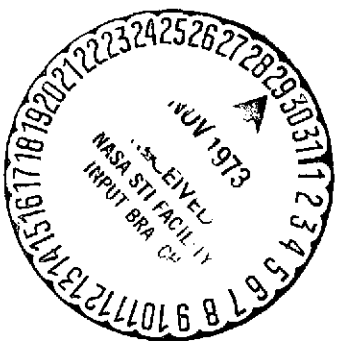

SKYLAB PLUME CONTAMINATION EXPERIMENTS

by Robert L. Bowman, Ernie W. Spisz, Ralph D. Sommers, and John R. Jack
Lewis Research Center
Cleveland, Ohio 44135

TECHNICAL PAPER proposed for presentation at Seventh Space Simulation cosponsored by the American Institute of Aeronautics, the American Society for Testing and Materials, and the Institute of Environmental Sciences
Los Angeles, California, November 12-14, 1973

SKYLAB PLUME CONTAMINATION EXPERIMENTS

by Robert L. Bowman, Ernie W. Spisz,
Ralph D. Sommers and John R. Jack

National Aeronautics and Space Administration
Lewis Research Center
Cleveland, Ohio

E-7397

ABSTRACT

The effects of combined exposure to RCS thruster exhaust products and simulated orbital solar radiation were measured on Skylab solar cells, S13G white thermal control coatings, a quartz sample, and a front surface aluminized mirror. A total of 75.5 seconds of exposure to 14 msec pulses from a 5 pound thrust MMH/N_2O_4 thruster was achieved. Solar cell maximum power was reduced as much as 10 per cent. The transmittance of the quartz decreased at all wavelengths between 0.2 and 2.5μm. The most significant transmittance decrease was found at the short wavelengths. For example at 0.2μm, the contaminated sample transmittance was reduced to zero. The mirror sample also showed a significant decrease in hemispherical reflectance at the short wavelengths The diffuse reflectance increased at all wavelengths. The S13G white coatings showed large changes in their optical properties. In-situ measurements of α_s and ϵ showed an average increase of 60 per cent in α_s and an average decrease of 15 per cent in ϵ after 58 seconds exposure to thruster firing. Ex-situ spectral measurements showed increases of 125 per cent in α_s after 75.5 seconds of exposure.

INTRODUCTION

The increasing complexity of space craft systems and longer duration missions have increased the possibility of spacecraft contamination which may compromise the operational characteristics of various experiments or critical spacecraft surfaces. A leading offender among the possible sources of contamination are the thrusters used for attitude control of the spacecraft. To illustrate the problem, figure 1 is a drawing of Skylab showing the areas which may be affected by the exhaust plumes from some of the thrusters used during docking and undocking maneuvers These areas include such items as solar cell panels, thermal control surfaces, and many experiment package windows and parts.

The effect of the contaminant on spacecraft optics, thermal control surfaces, and solar cells will be of concern if their respective functions are degraded by the deposition of contaminants upon them. In order to make reliable design calculations, information is required on the effects resulting from the thruster plume contamination and on the thruster plume mass deposition distribution.

A continuing research program is being conducted at the Lewis Research Center to determine the effects of exposure to rocket exhaust plumes on various spacecraft optical materials and critical surfaces (Ref. 1, 2, 3, 4, 5, 6, and 7). Recently a test was conducted at the request of the Skylab Project Office to determine: (1) the combined effects of thruster plume contamination and simulated solar radiation on typical Skylab surfaces and (2) the thruster plume mass flow distribution. The test was conducted in the Lewis Research Center's liquid helium cooled Environmental Simulator Facility with a 5 pound thrust bipropellant engine using MMH as a fuel and N_2O_4 as the oxidizer.

The effects of exposure to the thruster plume and solar simulation on Skylab solar cells, S13G white thermal control coatings, a quartz sample, and a front surface aluminized mirror will be presented in this paper. In addition, the results of an experiment included in this test to determine the possible effects of contamination from the test chamber are presented. The results of the plume mass distribution measurements are presented in reference 6.

EXPERIMENTAL PROCEDURE AND APPARATUS

Thruster and Facility Operations: The experiment was performed in the Lewis Research Center's 2 x 4 meter liquid helium cooled space simulation chamber (Figure 2) described in reference 1. A drawing of the horizontal test plane showing the thruster, sample pallet, samples, and other facility and test apparatus is shown in figure 3. The thruster used was a 5 pound thrust bipropellant engine using MMH as a fuel and N_2O_4 as oxidizer. It was operated in a pulsed mode, specified by the Skylab Project Office, of 14 msec ON time and 100 msec OFF time for a train of 25 consecutive pulses. In general, a pulse train was repeated every 7 minutes during a six hour testing period. The engine was fired on six days over a two week period, a total of 220 pulse trains was fired and 75.5 seconds of exposure during firing was accumulated.

A pressure of 1×10^{-9} torr is normally maintained in the vacuum facility with liquid helium cooled walls. In order to more effectively pump the hydrogen produced by the engine firings, a gaseous argon flow is introduced into the test section to cryotrap the hydrogen (see reference 1 for a discussion of this effect). The continuous argon flow raises the chamber pressure to a steady value of 5×10^{-7} torr. During the firing of each pulse train, the chamber pressure momentarily increases to approximately 5×10^{-5} torr then quickly returns to the original pressure of 5×10^{-7} torr.

At the conclusion of a firing day, the argon and liquid helium flows are turned off. The tank walls slowly warm and the cryotrapped hydrogen and condensed argon evaporate from the tank walls, renewing the simulator's cryopumping capability for further testing. During the approximately 4 hours required for warmup, momentary chamber pressures as high as 10^{-3} torr are recorded. In order to prevent evaporation of the lower vapor pressure combustion products, the tank wall temperatures were maintained below 100°K throughout the test by using cold helium gas (~20°K).

A carbon arc lamp was used to provide orbital solar radiation and was cycled 60 minutes on and 30 minutes off to simulate orbital conditions. The accumulated exposure (at approximately 95mw/cm^2) to simulated solar radiation was 63.5 Equivalent Sun Hours (ESH).

A 60 watt deuterium lamp was included within the vacuum chamber and was located 40 cm above the test plane as shown in figure 3 to provide supplemental ultraviolet radiation in the wavelength region from 0.2 to 0.3μm. The lamp was operated for 221 continuous hours providing a total exposure of 0.73 equivalent ultraviolet sun hours.

The solar cells, white thermal control coatings, and optical samples to be discussed in this report were mounted on a horizontal pallet (figure 3) located 10 cm below the thruster axis. All pallet samples were mounted with their top surfaces flush with the pallet surfaces in order to minimize exhaust flow disturbances.

Solar Cells. Six N/P silicon solar cells of the type used on Skylab were mounted on the sample pallet at the locations shown in figure 3. These cells were 2 x 2 cm with quartz cover plates having anti-reflection and ultraviolet protective coatings. The solar cells were not temperature controlled, the cells' temperature varied between 220°K with the arc lamp off and 320°K with the arc lamp on. Solar cell data were obtained when the cell temperatures were between 260°K and 290°K. Two radiometers, shown in figure 3, measured the light intensity in the test plane.

The current - voltage (I-V) characteristic curves were obtained in-situ periodically throughout the test. From the characteristic curves, the maximum power (P_{max}) output could be determined. Because slight differences in flux and temperature occurred throughout the test, it was necessary to normalize the P_{max} values for the intensity level and also to correct the data for temperature in order to obtain a valid comparison. The intensity normalization was accomplished by the parameter $P_{max}/Flux$. temperature correction was made by a linear fit of all of the $P_{max}/Flux$ with the temperature at which the data were obtained, and then correcting the $P_{max}/Flux$ values to 273°K ($(P_{max}/Flux)_N$).

Spectral Optical Properties. The spectral reflectances of the mirror sample (F, figure 3) and the S13G coatings (A and B, figure 3) were measured using a Gier-Dunkle MgO coated integrating sphere reflectometer (reference 8) with a Lithium Fluoride prism monochromator. The samples were mounted at the center of the integrating sphere. Either the angular-hemispherical or the diffuse reflectance was measured depending on the angle of incidence. The angular-hemispherical reflectance was measured for an angle of incidence of 15°, which is sufficiently close to normal incidence so that the measured reflectance is equal to the normal-hemispherical reflectance. Normal incidence is used to measure diffuse reflectance since the specular radiation is reflected out the entrance port of the sphere.

The integrating sphere system was also used to measure the spectral hemispherical transmittance of the quartz sample for the wavelength range from 0.34 to 2.5μm. With the sample located at the sphere entrance port the sample in/sample out technique yields the hemispherical transmittance.

In addition to the integrating sphere system, a one meter, 15^{o} Robin mount ultraviolet spectrometer was used for transmittance measurements the wavelength region from 0.2 to 0.5μm. Data were obtained for the sample mounted at both the entrance and exit slit. With the sample at the exit slit, the transmittance is nearly hemispherical since the detector senses most of the transmitted radiation. Measurements made with the sample mounted at the entrance slit yield directional transmittances since only the radiation transmitted along the optical axis of the spectrometer is measured, i.e. the scattered radiation is absorbed in the spectrometer The difference between the two types of measured transmittances is then due to scattered radiation.

White Thermal Control Coatings Two samples of S13G white thermal control coatings were located in positions A and B on the pallet as shown in figure 3. These samples were mounted and instrumented with thermocouples as described in reference 7. In-situ thermal optical property measurements of solar absorptance (α_s) and thermal emittance (ϵ) were made periodically during the test using the transient calorimetric technique described in reference 7. Briefly, this technique requires the sample to be heated by the solar simulator beam and then allowed to cool with the simulator off. Using both the heating and cooling curves, the solar absorptance and the thermal emittance can be calculated.

Test Chamber Effects The purpose of the thruster test was to measure the sample degradation due to rocket plume exhaust products alone. However, it was possible that the test chamber environment could also contaminate the samples and affect the test results. Two experiments were, therefore, included in this test to isolate extraneous sources of contamination from that of the thruster plume. One of these experiments was a quartz crystal microbalance (QCM) pointed away from the thruster so that any condensate forming on the crystal would either come from extraneous sources or from a plume reflection from the chamber walls.

The second experiment was a covered sample experiment containing two quartz discs mounted (figure 3) in a horizontal plane with their top surface at pallet elevation. Sample 1 was covered at all times except for a period of 30 seconds during which the thruster was fired. The cover was removed from sample 1 ten seconds before engine firing and replaced twenty seconds after engine fire. Thus, this sample was primarily exposed to contamination only from the thruster plume. Sample 2 was exposed throughout the two week test period. Ex-situ transmittance measurements were made on the samples at the end of the test to compare the optical effects due to the different exposures.

The QCM was located in the test plane at pallet elevation (figure 3). The crystal faced away from the thruster and was inclined at an angle of 45^{o} below the horizontal. The crystal has a diameter of 1.25 cm and a natural oscillating frequency of 5×10^{6} Hz Since the crystal frequency is dependant on

temperature as well as on the net mass deposited, the QCM was water cooled to minimize the temperature variations. The frequency sensitivity of the QCM system is 1 Hz which corresponds to a mass change of 1.8×10^{-8} gm/cm^2

RESULTS AND DISCUSSION

Solar Cells. Figure 4 shows typical characteristic curves for solar cell 1 (figure 3) taken for zero and 75.5 seconds of exposure to the thruster plume The I-V characteristics showed no change in shape due to the combined exposure. The light generated current did decrease indicating that the decrease in performance is due to a decrease in transmittance of the cover plate caused by contaminant absorptance.

Figures 5a and 5b show the corrected maximum power ($(P_{max}/Flux)_N$) versus thruster exposure time for solar cells 1 and 2. For both cells $(P_{max}/Flux)_N$ gradually decreases with exposure time. After 75 5 seconds of exposure, $(P_{max}/Flux)_N$ had decreased 8 and 7 per cent for solar cells 1 and 2 respectively. The remaining three cells for which data were obtained (cells 4, 7, and 8; figure 3) also showed the gradually decreasing trend with total changes varying between 5 and 10 per cent. A decrease of this magnitude might be significant especially if the expected decrease due to radiation damage also occurs.

Spectral Optical Properties. The effect of 75.5 seconds exposure to the thruster plume and solar simulation on the transmittance of quartz sample E (figure 3) is shown in figure 6 for the wavelengths between 0.2 and 0.6μm. The measured hemispherical and directional transmittances between 0.2 and 0.6μm are about the same. This similarity indicates that the transmittance change is primarily due to contaminant absorption although some minor scattering effects may be present. A significant decrease in transmittance can be seen for wavelengths less than 0.5μm. At 0.2μm, for example, the contaminated transmittance is 0.0 compared to 0.9 for the clean sample. Since many space experiments involve ultraviolet measurements which cannot be made from the ground due to atmospheric absorption at the short wavelengths, the large transmittance losses obtained at these wavelengths are of concern. The hemispherical spectral transmittance for the clean and contaminated quartz sample from 0.4 to 2.5μm is shown in figure 7. From this figure and figure 6, it can be seen that the major changes in transmittance occur at wavelengths less than 0.6μm. However, changes in transmittance of 2 to 4 per cent occur at wavelengths as long as 2.5μm.

A comparison can be made between the change in spectral directional transmittance of quartz from this test and the results from an earlier test (reference 4) using the same thruster. In the previous test, the thruster was fired in a pulsed mode with 50 msec On time and 100 msec OFF time for a string of 8 consecutive pulses. A total thruster exposure time of 223.7 seconds was accumulated with no solar simulation. Directional transmittance ratios (contaminated sample transmittance/clean sample transmittance) for the quartz samples in similar locations from both tests are shown in figure 8. This figure

shows that the optical transmittance degradation resulting from a total exposure of 75.5 seconds to 14 msec pulses with orbital simulation is considerably more severe than that resulting from a total exposure of 223.7 seconds to 50 msec pulses without solar simulation. Previous experiments (Reference 1) indicate that pulse times of less than 35 msec for this thruster are insufficient for complete combustion. We suspect the primary cause of the severe degradation at the shorter wavelengths to be incomplete combustion products. A secondary cause we believe to be the ultraviolet radiation present in the solar simulation since ultraviolet radiation is known to polymerize many chemical compounds. Further experimentation is required in order to separate these two effects.

As stated previously, the solar cell data indicated that the loss in performance was due to a decrease in transmittance of the cover plate. To further check this result, the quartz sample spectral hemispherical transmittance data was used to calculate the fractional change in the total power output due to a change in transmittance. The fractional change in power was calculated by

$$\frac{P_{clean} - P_{contaminated}}{P_{clean}} = 1 - \frac{\int \tau_c(\lambda) R(\lambda) \phi(\lambda) d\lambda}{\int \tau(\lambda) R(\lambda) \phi(\lambda) d\lambda}$$

where $\tau_c(\lambda)$ is the hemispherical transmittance of the contaminated sample, $\tau(\lambda)$ is the hemispherical transmittance of the clean sample, $R(\lambda)$ is the relative spectral response of the solar cell, and $\phi(\lambda)$ is the spectral irradiance of the carbon arc lamp. This calculation yielded a 6 per cent reduction in the power output due to the change in transmittance. This value is consistent with the measured average solar cell maximum power decrease of 7 per cent indicating that the solar cell power degradation was indeed due to a loss of cover plate transmittance cuased by the contaminant.

The effect of the combined exposure on the spectral hemispherical and diffuse reflectance of a front surface aluminized mirror (sample F, figure 3) is shown in figure 9. A considerable decrease in the hemispherical reflectance is found at wavelengths less than 0.7μm. At 0.35μm, for example, the reflectance of the contaminated mirror is 0 25 compared to 0.81 for the clean mirror. The loss of reflectance at the short wavelengths could be a severe problem in an ultraviolet sensitive system. Between 0.8 and 1.5μm, a small increase in the hemispherical reflectance (about 4 per cent at 1.0μm) can be seen. For wavelengths longer than 1.5μm relatively little difference is found. Also shown in the figure is the diffuse reflectance of the contaminated mirror. Since the measured diffuse reflectance of the clean sample is zero, the curve shows an increase in the diffuse reflectance of 0.03 to 0.08 over the wavelength region from 0.5 to 1.5μm. This could cause a loss of resolution if the mirror is used in an imaging type of system.

A comparison of the change in hemispherical reflectance of the mirror from 75.5 seconds of exposure with that obtained with 223.7 seconds of exposure previously reported (Reference 4) can also be made. As was found from the

transmittance comparison, there was considerably more degradation from the short pulse test with solar simulation than there was from the longer pulse test with no solar simulation.

S13G WHITE COATINGS: In-situ α_s and ϵ measurements for the two S13G samples (samples A and B, Figure3) are shown in figure 10. These measurements showed an average increase in α_s of 60 per cent. The average emittance decreased by 15 per cent. Thus the α_s/ϵ ratio increased by an average of 90 per cent. These changes were obtained after 58 seconds of exposure to thruster firing. Data could not be taken through to the end of the test (75.5 seconds of exposure) because of data recording equipment malfunction.

A previous in-situ rocket damage test has been made during which 223.7 seconds of plume exposure to 50 msec pulses was accumulated with no solar simulation. A comparison of the short and long pulse damage to S13G has been reported (Reference 5). But in brief, it is noted that the short pulse test damage reported herein is not only greater than that measured for the long pulse test, but the greater damage occurred for a much shorter exposure time. After 223.7 seconds of exposure to the long pulse exhaust, α_s increased by 25 per cent and ϵ was unaffected. The α_s/ϵ ratio thus increased by 25 per cent.

The visual appearance of the coatings changed considerably after exposure to the rocket plume. Initially the coatings are white. Exposure to 223.7 seconds to the long pulse length changed the coatings to a light tan color. Exposure to only 75.5 seconds of the short pulse length caused the coatings to become a light brown. These color changes are consistent with the various measured changes in solar absorptance of these coatings.

The short pulse test data reported here exposed the samples to extensive solar radiation, including the short wavelength part of the spectrum. Thus a possible interaction between the S13G, ultraviolet, and rocket exhaust deposits may account for the more rapid damage during the short pulse test. In addition, it should be recalled that the operation of the rocket is less efficient in the short pulse mode and this allows more unburned propellants to be expelled in the rocket exhaust.

Ex-situ spectral reflectance measurements were made before and after exposure to the 14 msec pulses and the solar simulation. The spectral reflectances are shown in figures 11a and 11b. The largest changes occur between 0.4 and 0.6μm. Since this wavelength range corresponds to the peak of the solar irradiance, large changes in solar reflectance would be expected. The solar reflectance (ρ_s) can be calculated by integrating the spectral hemispherical reflectance with respect to the solar spectral irradiance. The solar absorptance can then be calculated as ($\alpha_s = 1 - \rho_s$) This calculation yields an increase of 145 and 103 per cent for the two samples after 75.5 seconds of exposure. This is more change than was found from the in-situ measurements (60 per cent increase in α_s) for 58 seconds of exposure. The greater damage shown for the ex-situ measurements is possibly due to the longer exposure, i.e., 75.5 compared to 58 seconds.

TEST CHAMBER EFFECTS: The spectral hemispherical transmittances for the samples from the covered sample experiment are shown in figure 12. Only the transmittances for wavelengths below 0.6μm are shown since this region is the most sensitive to contamination effects. Only a slight difference is seen between the sample exposed only during thruster firing periods (sample 1) and the sample which was always exposed (sample 2). This indicates that significant contamination occurs only during engine firing periods and that there are no significant extraneous sources of contamination affecting optical characteristics. The QCM, which was used to monitor events occurring during non-firing periods, showed within the limits of its measurement capability no mass deposition during the test.

SUMMARY OF RESULTS

The effects of combined exposure to thruster exhaust products and simulated orbital solar simulation were measured on Skylab solar cells, S13G white thermal control coatings, a quartz sample, and a front surface mirror.

Solar cell maximum power was reduced by 5 to 10 per cent. The degradation was found to be due to a loss of cover plate transmittance due to the contaminant. A power loss of 6 per cent was calculated from the measured hemispherical transmittance of the quartz sample. This compared closely with the average power loss of 7 per cent measured on the solar cells in situ.

The quartz sample showed a decrease in transmittance for all wavelengths between 0.2 and 2.5μm. The largest decrease was found for wavelengths less than 0.5μm. For example, at 0.2μm the contaminated transmittance reduced to zero while that for the clean sample was 0.9. The large loss of transmittance could be a major concern in ultraviolet measuring systems. The degradation of quartz transmittance from two different tests were compared. The transmittance degradation obtained from the 14 msec pulse test (75.5 seconds total exposure) with orbital solar simulation was much greater than that noted for the previously reported 50 msec test (223.7 seconds total exposure). This indicated that the 14 msec pulse may be considerably more contaminating due to the more incomplete combustion process and also that a contaminant-ultraviolet interaction may be present.

The contaminated mirror showed a decrease in hemispherical reflectance at short wavelengths. A reflectance of 0.25 compared with a clean mirror reflectance of 0.81 was measured at 0.35μm. In addition, the diffuse reflectance increased from 0.0 to 0.8 at 0.6μm. These changes could be of concern in ultraviolet systems and also in imaging systems where resolution is important. The mirror results also indicated more degradation from this test than from the earlier test with longer pulse width and no solar simulation.

The S13G white paints underwent large changes in their optical properties. In-situ measurements of α_s and ϵ showed 60 per cent increase in α_s and 15 per cent decrease in ϵ after 58 seconds exposure to thruster firing. The ex-situ before and after spectral measurements showed increases of 145 and 103 per cent in α_s for 75.5 seconds of exposure. The largest changes in spectral reflectance occurred in the wavelength range between 0.4 and 0.6μm.

The results of the experiments to determine the effects of the test chamber environment indicated there are no significant sources of contamination except the thruster.

REFERENCES

1. Cassidy, J. F., "Space Simulation Experiments on Reaction Control System Thruster Plumes", AIAA Paper 72-1071, New Orleans, La., 1972.

2. Jack, J. R., Spisz, E. W., and Cassidy, J. F., "The Effect of Rocket Plume Contamination on the Optical Properties of Transmitting and Reflecting Materials", AIAA Paper 72-56, San Diego, Calif., 1972.

3. Spisz, E. W., Bowman, R. L., and Jack, J. R., "Exhaust Plume and Contamination Characteristics of a Bipropellant (MMH/N204) RCS Thruster", 7th JANNAF Plume Technology Conference, Redstone Arsenal, Ala., April 1973, TM X-68212, 1973, NASA.

4. Bowman, R. L., Spisz, E. W., and Jack, J. R., "Effect of Contamination on the Optical Properties of Transmitting and Reflecting Materials Exposed to a MMH/N204 Rocket Exhaust", 7th JANNAF Plume Technology Conference, Redstone Arsenal, Ala., April 1973, TM X-68204, 1973, NASA.

5. Sommers, R. D., and Raquet, C. A., "Effect of Thruster Pulse Length Thruster-Exhaust Damage of S13G White Thermal Control Coatings", 7th JANNAF Plume Technology Conference, Redstone Arsenal, Ala., April 1973, TM X-68213, 1973, NASA.

6. Spisz, E. W., Bowman, R. L., and Jack, J. R., "Plume Mass Flow and Damage Distributions for an MMH/N_2O_4 RCS Thruster", Paper presented at 7th AIAA/ASTM/IES Space Simulation Conference, Los Angeles, Cal., Nov. 1973.

7. Sommers, R. D., Raquet, C. A., and Cassidy, J. F., "Optical Properties of Thermal Control Coatings Contaminated by a MMH/N_2O_4 5-pound Thruster in a Vacuum Environment with Solar Simulation", Thermal Control and Radiation, vol. 31 of Progress in Astronautics and Aeronautics, Chang-Lin, Tien, ed., MIT Press, 1973, pp 145-158, also AIAA Paper 72-263, San Antonio, Texas, 1972.

8. Edwards, D. K., Gier, J. T., Nelson, K. E., and Roddick, R. D., "Integrating Sphere for Imperfectly Diffuse Samples", Journal of the Optical Society of America, vol. 51, No. 11, Nov. 1961, pp 1279-1288.

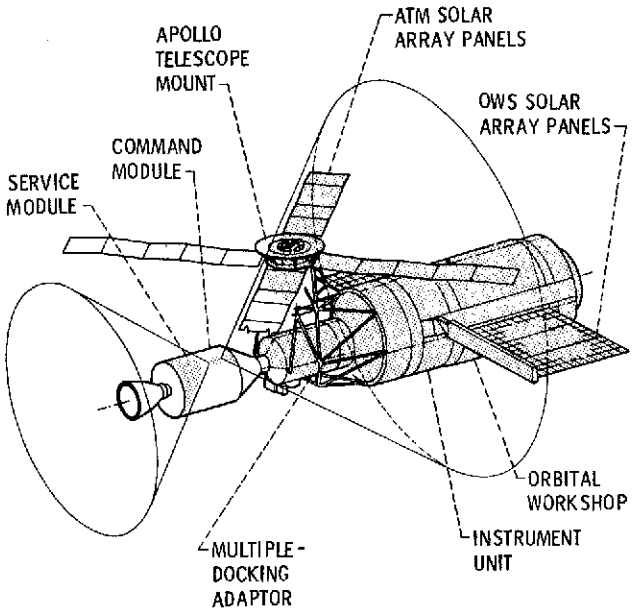

Figure 1. - Skylab drawing with shaded areas indicating regions of possible exhaust plume contamination.

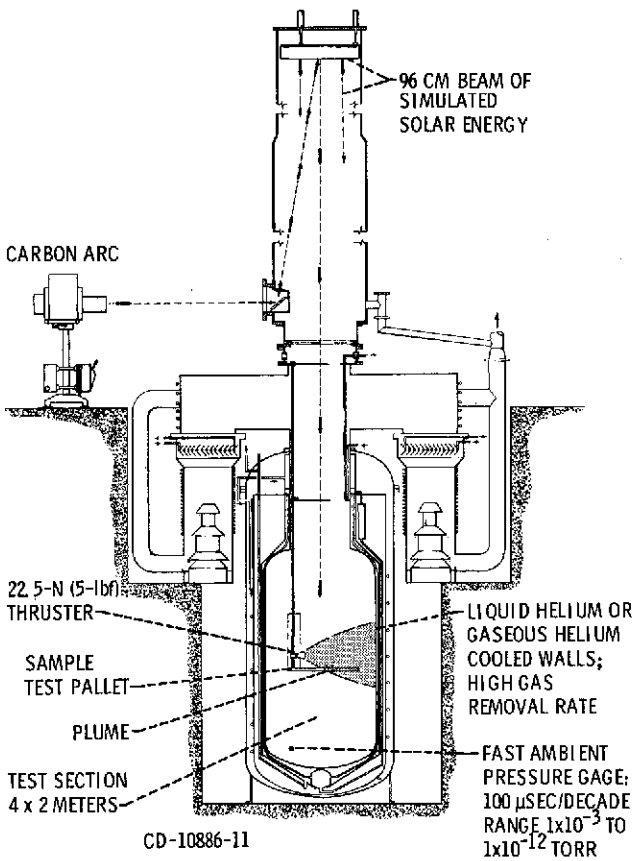

Figure 2. - Liquid helium cooled space simulator and thruster installation.

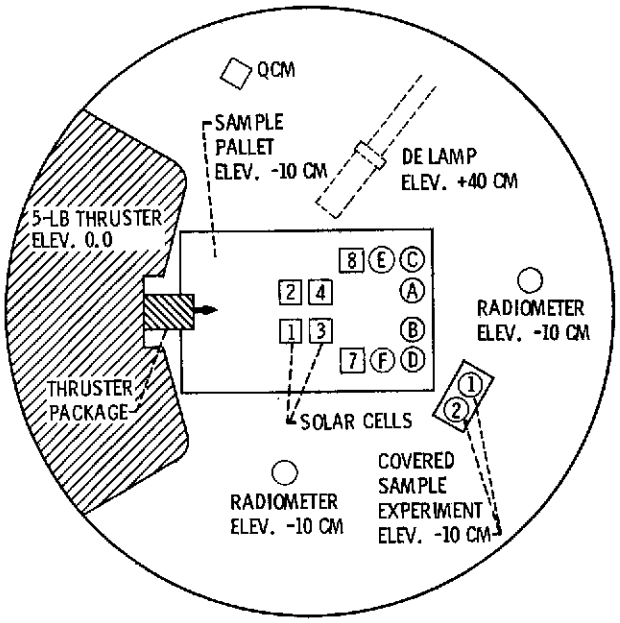

Figure 3. - Skylab experiment package layout.

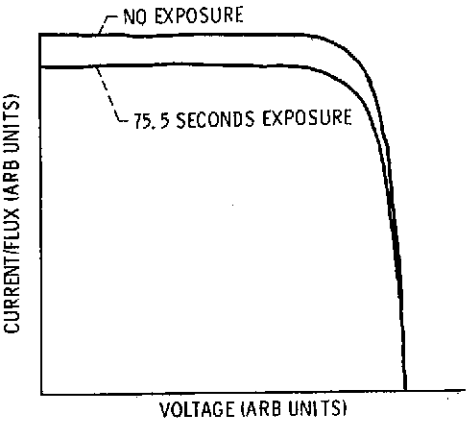

Figure 4. - Solar cell characteristic curves before and after exposure to the thruster plume.

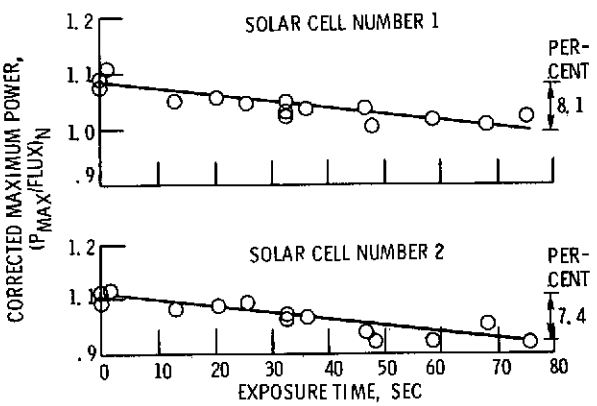

Figure 5. - Effect of combined exposure on solar cell maximum power output.

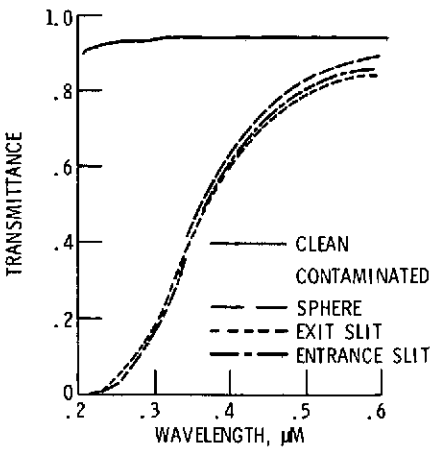

Figure 6. - Effect of the combined exposure on the spectral transmittance of quartz.

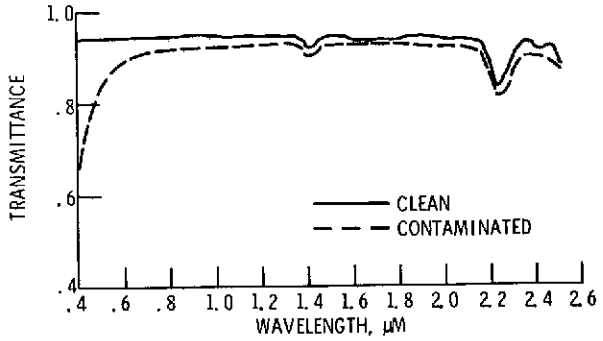

Figure 7. - Effect of the combined exposure on the spectral transmittance of quartz.

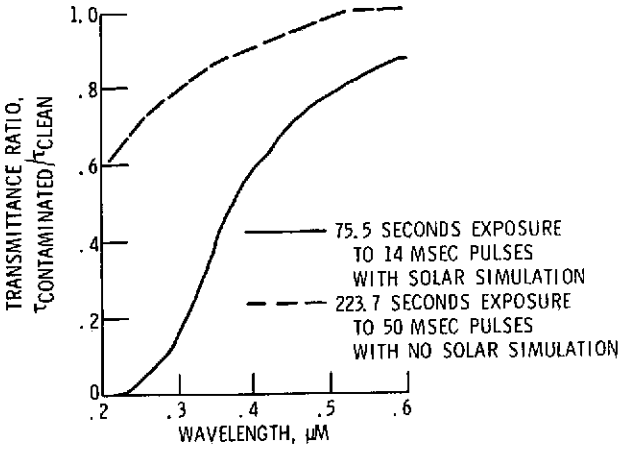

Figure 8. - Quartz sample transmittance ratios for two different exposures.

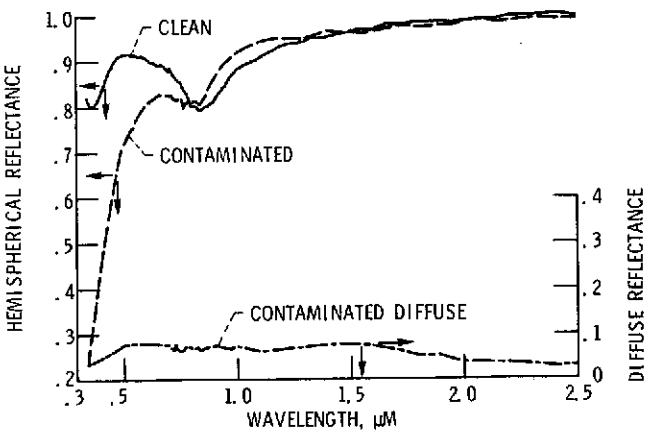

Figure 9. - The effect of the combined exposure on the spectral reflectance of a front surface mirror.

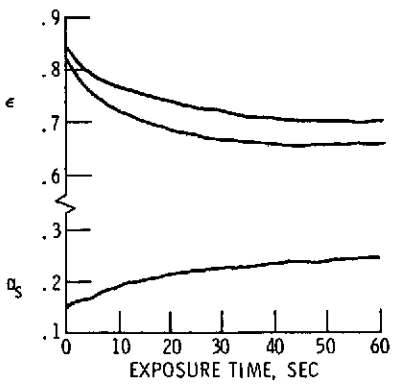

Figure 10. - Changes in thermal emittance and solar absorptance of S13G white coatings.

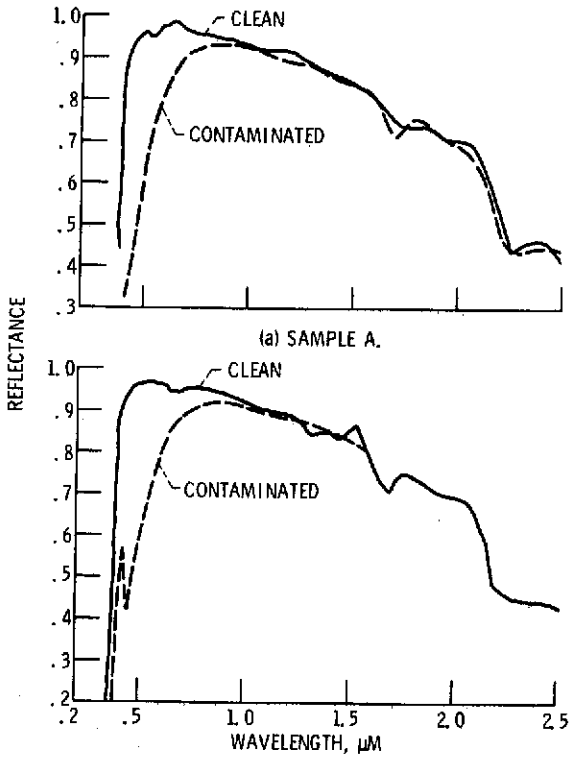

Figure 11. - The effect of the combined exposure on the spectral reflectance of S13G white coatings.

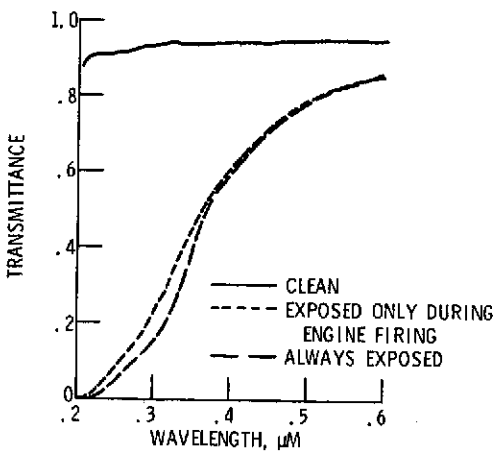

Figure 12. - Spectral transmittance of quartz from covered sample experiment.